HHS Public Access

Author manuscript

Acad Radiol. Author manuscript; available in PMC 2016 July 01.

Published in final edited form as:

Acad Radiol. 2015 July ; 22(7): 840–845. doi:10.1016/j.acra.2015.03.001.

Multimodality 3D Tumor Segmentation in HCC patients treated with TACE

Zhijun Wang, M.D,PhD[1,2], **Julius Chapiro, M.D**[1], **Rüdiger Schernthaner, M.D**[1], **Rafael Duran, M.D**[1], **Rongxin Chen, M.D, PhD**[1], **Jean-François Geschwind, M.D**[1], and **MingDe Lin, PhD**[3]

[1]Russell H. Morgan Department of Radiology and Radiological Science, Division of Vascular and Interventional Radiology, The Johns Hopkins Hospital, Sheikh Zayed Tower, Ste 7203, 1800 Orleans St, Baltimore, MD, USA 21287

[2]Interventional Radiology Department, Chinese PLA General Hospital 28 Fuxing Road, Haidian District, Beijing, China, 100853

[3]U/S Imaging and Interventions (UII), Philips Research North America, Briarcliff Manor, NY, USA

Abstract

Rationale and Objectives—To validate the concordance of a semi-automated multimodality lesion segmentation technique between contrast-enhanced MRI (CE-MRI), cone-beam CT (CBCT) and multi-detector CT (MDCT) in patients with hepatocellular carcinoma (HCC) treated with transarterial chemoembolization (TACE).

Materials and methods—This retrospective analysis included 45 patients with unresectable HCC that underwent baseline CE-MRI within one month before the treatment, intraprocedural CBCT during conventional TACE and MDCT within 24 hours post TACE. Fourteen patients were excluded due to atypical lesion morphology, portal vein invasion or small lesion size which precluded sufficient lesion visualization. 31 patients with a total of 40 target lesions were included into the analysis. A tumor segmentation software, based on non-Euclidean geometry and theory of radial basis functions, was used to allow for the segmentation of target lesions in 3D on all three modalities. The algorithm created image-based masks located in a 3D region whose center and size was defined by the user, yielding the nomenclature “semi-automatic”. Based on that, tumor volumes on all three modalities were calculated and compared using a linear regression model (R^2 values). Residual plots were used to analyze drift and variance of the values.

Correspondence to Jean-François Geschwind, M.D., Professor of Radiology, Surgery and Oncology, Tel: 410-614-2648 (office), 410-955-0233(Fax), jfg@jhmi.edu..
The information for each contributing author:
Zhijun Wang, M.D&PhD, wangzj301hospital@163.com
Julius Chapiro, M.D, j.chapiro@googlemail.com
Rüdiger Schernthaner, M.D, rschern1@jhmi.edu
Rafael Duran, MD, rafaelduran.md@gmail.com
Rongxin Chen, M.D&PhD, rongxinchen99@126.com
MingDe Lin, PhD, ming.lin@philips.com

Results—The mean value of tumor volumes was 18.72±19.13cm^3 (range, 0.41-59.16cm^3) on CE-MRI, 21.26±21.99 cm^3 (range, 0.62-86.82 cm^3) on CBCT and 19.88±20.88 cm^3 (range, 0.45-75.24 cm^3) on MDCT. The average volumes of the tumor were not significantly different between CE-MR and DP-CBCT, DP-CBCT and MDCT, MDCT and CE-MR (p=0.577, 0.770 and 0.794 respectively). A strong correlation between volumes on CE-MRI and CBCT, CBCT and MDCT, MDCT and CE-MRI was observed (R^2=0.974, 0.992 and 0.983, respectively). When plotting the residuals, no drift was observed for all methods showing deviations of no more than 10% of absolute volumes (in cm^3).

Conclusion—A semi-automated 3D segmentation of HCC lesions treated with TACE provides high volumetric concordance across all tested imaging modalities.

Keywords

Tumor segmentation; MRI; C-arm cone beam CT; MDCT; hepatocellular carcinoma; TACE

INTRODUCTION

Locoregional therapies (i.e. conventional transarterial chemo-embolization [cTACE]) represent the mainstay of therapy for patient with unresectable primary and some secondary liver malignancies. Because treatment recommendations are usually based on measurements made on cross-sectional imaging, accurate and workflow-efficient evaluation of tumor size on baseline imaging as well as radiological tumor response assessment on follow-up imaging constitute important aspects of the therapeutic concept(1-3). There are three accepted methods to assess tumor response to TACE: Response Evaluation Criteria in Solid Tumor [RECIST], European Association for the Study of the Liver [EASL] guidelines and modified RECIST [mRECIST]. The diameter-based RECIST is used to measure changes in overall tumor size. The bi-dimensional EASL is used to measure the area of enhancement and the more recently introduced uni-dimensional mRECIST measures the maximal diameter of tumor enhancement(4, 5).The advent of workflow-efficient and clinically practicable segmentation-based 3D quantification of tumor volumes has been confirmed as technically feasible, highly reproducible and reader independent. However, no evidence exists until today for the inter-modality concordance between these systems. Prior to their full clinical introduction, these methods must be shown as accurate and reproducible across all cross-sectional imaging modalities. The purpose of this study was thus to validate the concordance of a semi-automated multimodality lesion segmentation technique on contrast-enhanced MRI (CE-MRI), C-arm cone-beam CT (CBCT) and multi-detector CT (MDCT) in patients with hepatocellular carcinoma (HCC) treated with transarterial chemoembolization.

MATERIAL AND METHODS

Patient Study Selection

This was a single institution retrospectively study. Health Insurance Portability and Accountability Act compliant and institutional review board were approved. All patients were provided with informed consent before cTACE in the study. Diagnosis of HCC was confirmed by liver biopsy or the lesion presented with typical features on dynamic contrast-

enhanced CT or MR cross-sectional imaging (hypervascularity in the arterial phase and washout in the venous phase) and an alpha-fetoprotein level of 200 ng/mL or higher. Patients with unresectable HCC were evaluated and treated with conventional TACE (cTACE) after discussion at the multidisciplinary liver tumor conference. Eligibility criteria for cTACE were as follows: focal or multifocal unresectable HCC; Child-Pugh classification A or B; Eastern Cooperative Oncology Group performance status 0 or 1, and no contraindication to contrast medium. The patients with tumor burden of greater than 70% presence of extrahepatic disease, or complete tumor occlusion of the portal vein were excluded. The eligibility criteria for assessment of the treated target lesions included all patients: 1) with dynamic contrast-enhanced MRI (CE-MRI) within 4 weeks before cTACE, intraprocedural dual phase CBCT (DP-CBCT) and MDCT 24 hours after cTACE; 2) Target lesion was visualized well in all the three modalities; 3) Clear border between tumor and liver tissue. Targeted lesions that were not visualized well (i.e. atypical lesion morphology like that found in infiltrative disease) or with insufficient imaging on either modality were excluded from this study.

Preprocedural CE-MRI Technique

All patients underwent baseline CE-MRI imaging using a 1.5-T MR unit (CV/I, GE Medical Systems, Milwaukee, WI) and a phased-array torso coil within 4 weeks before the TACE. The imaging protocol included: 1) axial T2-weighted fast spin-echo images (repetition time [TR]/echo time [TE], 5000/100 msec; matrix size, 256 × 256; slice thickness, 8 mm; interslice gap, 2 mm; receiver bandwidth, 32 kHz); 2) axial single-shot breath-hold gradient-echo diffusion weighted echo-planar images (TR/TE, 5000–6500/110 msec; matrix size, 128x128; slice thickness, 8 mm; inter slice gap, 2 mm; b value, 500 second/mm2; receiver bandwidth, 64 kHz); and 3) axial breath-hold unenhanced and contrast-enhanced (0.1 mmol/kg intravenously of gadodiamide, Omniscan, General Electric, Princeton, NJ) T1-weighted three-dimensional fat-suppressed spoiled gradient-echo images (TR/TE, 5.1/1.2 m sec; field of view, 320–400 mm2; matrix size, 192 × 160; slice thickness, 4–6 mm; receiver bandwidth, 64-kHz; flip angle, 15) in the arterial and portal venous phases (20 and 70 seconds after intravenous contrast administration, respectively). The arterial and venous phase of the CE-MRI imaging was used for the study.

Intraprocedural Dual Phase CBCT Technique

The intrprocedural dual phase CBCT was performed to visualize the target lesion and its feeding arteries before chemoembolization. The imaging was performed using a commercially available angiographic system (Allura Xper FD20, Philips Healthcare, Best, The Netherlands). This system was equipped with the XperCT option, enabling C-arm CBCT acquisition and volumetric image reconstruction (Feldkamp back projection). For each CBCT scan, the area of interest was positioned in the system isocenter, and over approximately 5 seconds, 312 projection images (60 frames per second) were acquired with the motorized C-arm covering a 200° clockwise arc at 40° per second rotation speed (matrix size, 384 × 384 × 296; field of view, 25 × 25 × 19 cm). As the images were being acquired, the projections were transferred to the reconstruction computer to produce volumetric data. 0.6mm isotropic images were reconstructed from the DP-CBCT scans. The dual-phase prototype feature allowed for the acquisition of two sequential multiphasic CBCT scans

using only one contrast injection. The same contrast injection protocol was applied to all cases: the contrast injection was done through the catheter placed into the proper hepatic artery, and the scan was trigged after contrast was injected for 3 seconds (amount 18 mL; rate 2 mL/s; Oxilan 300 mgI/mL, Guerbet LLC, Bloomington, IN). The patients were instructed to be at end-expiration apnea during each of the CBCT scans with free breathing between the early and delayed arterial phase scans. If needed, oxygen was administered to patients during the acquisition to minimize the discomfort of breath holding. In this work, the second phase was used because the tumors were best visualized at that phase (6, 7).

Transcatheter Arterial Chemoembolization

cTACE was performed according to our standard institutional protocol, and all procedures were performed by an interventional radiologist (XYZ) with 15 years of experience in hepatic interventions. With use of the Seldinger's technique, a 5-F vascular sheath was placed in the right common femoral artery over a 0.035-inch guide wire (Terumo Medical, Somerset, NJ). Under fluoroscopic guidance, a 5-F glide Simmons-1 catheter (Cordis, Miami, FL) was advanced into the aortic arch and then used to select the celiac axis. The catheter was advanced into the desired hepatic artery over the guide wire. Using a 3-F Renegade High-Flo catheter coaxially over a 0.014-inch Transcend wire (Boston Scientific, Natick, MA), selective catheterization was performed to achieve lobar or segmental chemoembolization. A solution containing 50 mg doxorubicin (Adriamycin; Pharmacia &Upjohn, Peapack, NJ), and 10 mg mitomycin C in a 1:1 mixture with lipiodol (Lipiodol; Guerbet, Paris, France) was infused and followed by the infusion of gelatin-coated trisacryl microspheres (Embosphere particles; Biosphere Medical, Rockland, MA) until arterial inflow was retarded as seen on fluoroscopy.

MDCT Technique

Unenhanced MDCT was performed 24 hours after cTACE with a multislice CT scanner (Sensation 64; Siemens Medical Solutions, Erlangen, Germany) using a standard abdominal scan protocol as described. The scanning parameters were the following: 120 kVp, 545 mA; scan speed, 0.33 sec/revolution; detector collimation, 0.6 mm/row; helical pitch factor, 0.575/revolution. Images were then reconstructed using body kernel B30f, with a 400 × 400 × 220 mm field of view (matrix size 512 × 512 × 300) with a voxel size of 0.78 mm^3.

Semiautomatic Tumor Segmentation

A quantitative and 3D tumor segmentation software, based on non-Euclidean geometry and theory of radial basis functions (Medisys, Philips Research, Suresnes, France) was used to allow for the segmentation of target lesions in 3D on all three modalities. This method allows segmentations that follow 3D image features, including straight edges and corners. The algorithm used is based on the linear combination of image dependent shapes. Each shape is built on the basis of image features located in a 3D region whose center and size are specified by the user. In actual usage, the segmentation is an interactive, real-time process where the user expands/contracts the segmentation volume by a mouse click followed by a mouse drag (8). The combination of the segmentation shape construction is done through the optimization of an image-based criterion (eg, maximizing the gradient flow through the boundary of the combination). Moreover, the user can constrain the algorithm to include or

exclude a new segmentation shape (defined by a new point and size), thus freely controlling the final aspect of the global segmentation combination. This method was used because it can accurately segment in three dimensions with minimal user interaction. This semiautomatic segmentation method can accurately segment in three dimensions and has high reproducibility (validated to pathology in an animal model, and having a Dice similarity coefficient > 0.7 in clinical evaluation) and workflow efficiency (<2 minutes to segment a lesion in 3D) as previously reported (9,10). In our study, two radiological readers (YY - 10 years' experience, and ZZ - 15 years' experience.) selected and assessed the target lesions to which the segmentation was then performed (Figure 1).

Statistical Analysis

The tumor volumes resulting from the segmentations between CE-MR and DP-CBCT, CBCT and MDCT, CE-MRI and MDCT were compared using the two-tailed Student's t-test for paired data. A p-value ≤ 0.05 was considered statistically significant. The tumor volumes resulting on all analyzed modalities (CE-MRI, DP-CBCT and MDCT) were also compared using a linear regression model. Pearson's correlation coefficients (R^2) were calculated to compare the values between CE-MRI and CBCT, CBCT and MDCT, and CE-MRI and MDCT. Residual analysis was performed for each method and were plotted to analyze drift and variance of the values. Data analysis was performed using SPSS 15.0 (SPSS, Chicago, IL).

RESULTS

Patient Demographics

From April, 2012, and February, 2014, the liver tumor board discussed the care of 64 patients who had HCC and who had fulfilled the cTACE inclusion criteria. Of 64 patients, 45 patients underwent preprocedural CE-MRI within one month before the treatment, intraprocedural DP-CBCT during TACE and MDCT within 24 hours post TACE. Fourteen patients were excluded due to atypical lesion morphology, hepatic arterioportal fistula or small lesion size which precluded sufficient lesion visualization. 31 patients were included in this study. There were twenty-six men and five women with a mean patient age of 63.90±9.50 years (range, 44-81 years). A total of 40 target lesions (mean lesions per patient, 1.3; range, 1-3 lesions) were included into the analysis.

Tumor Volume on Preprocedural CE-MRI, DP-CBCT and MDCT

The mean value of tumor volumes was 18.72±19.13cm^3 (range, 0.41-59.16cm^3) on pre-procedural CE-MRI, 21.26±21.99 cm^3 (range, 0.62-86.82 cm^3) on DP-CBCT and 19.88±20.88 cm^3 (range, 0.45-75.24 cm^3) on MDCT. As shown in Table 1, the average volumes of the tumor were not significantly different between CE-MR and DP-CBCT, DP-CBCT and MDCT, MDCT and CE-MR (p=0.577, 0.770 and 0.794 respectively). A strong correlation between volumes was observed on pre-procedural CE-MRI and DP-CBCT, DP-CBCT and MDCT, MDCT and pre-procedural CE-MRI (Linear regression correlation coefficient: R^2=0.974, 0.992 and 0.983 respectively; (Figure 2). When plotting the residuals, no drift was observed for all methods showing deviations of no more than 10% of absolute volumes (in cm^3; Figure 2).

DISCUSSION

This study demonstrates a strong correlation between segmentation-based tumor volumes acquired on CE-MRI, CBCT and MDCT. Our study shows that 3D semiautomatic tumor volume segmentation software provides high volumetric concordance across all tested imaging modalities.

Tumor volumetric measurement using 3D tumor segmentation software may be a more accurate method than one-dimensional and two-dimensional measurement methods (9-11) . Importantly, volumetric techniques were shown to have a strong influence on how tumor response is classified and in some studies, the classification of patients as responders or non-responders was shown to differ between 3D and non-3D techniques in up to one-third of the analyzed cases (12, 13). Furthermore, 3D quantitative techniques have been repeatedly shown as beneficial in identifying tumor response more accurately, primarily because they include the whole tumor tissue into the analysis (14, 15) . For assessment of radiological response after TACE, 3D volumetric measurement has a strong clinical impact to be able to accurately measure what part of the lesion is necrotic and viable(16).

Specifically, there are several semi-automated segmentation techniques that have been described for 3D tumor analysis (9, 20). Region-growing algorithms are the most common approaches in use which is based on the linear combination of image-dependent shapes. Each shape is built on the basis of an image's features located in a 3D region whose center and size are specified by the user. These shapes are combined through the optimization of an image-based criterion. The user can constrain the algorithm to include or exclude a new shape and freely controls the final aspect of the global combination. Semi-automated techniques allow for combining the benefits of software-assisted workflow efficiency (less time) with reader input for accuracy. As opposed to that, manual segmentation needs more time, a high level of expertise and good knowledge of image features for accuracy (21). Generally, for a capable tumor segmentation software, it needs to take into account the complex appearances of tumors, neighboring structures, variable degrees of enhancement, and adjacent artifacts. In the present study, the tumor volume segmentation software was successfully used to segment tumors with three imaging modalities.

In our previous study, we showed the accuracy of volumetric tumor measurement as well as semiautomatic quantification of tumor enhancement (viable tissue) for hepatocellular carcinoma lesions after TACE (9). Furthermore, the utilized software was shown to be reproducible, anatomically precise and showed a high inter-reader concordance. However, the ability of such semi-automated segmentation techniques to provide reliable inter-modality measurements has not yet been demonstrated. This study addressed this paucity of data and validates the concordance of 3D quantitative, semi-automatic segmentation of hepatic tumor volume across the most commonly used, cross-sectional imaging modalities including CE-MRI, DP-CBCT and MDCT. The results in our study demonstrated that a 3D semiautomatic tumor volume segmentation can provide high volumetric accuracy across all tested imaging modalities. This result has a potential important clinical significance. It provides the foundation for a volumetric characterization of HCC lesions in the setting of TACE, before and after therapy.

There are some limitations. First, there were a relatively small number of patients, and this is because only some patients received imaging in all three modalities. A large population study could help to mitigate any bias due to patient size. Second, only HCC lesions that had clear borders (not diffuse/infiltrative disease) were included in this study. In future work, using whole liver 3D segmentation could solve this limitation, and the performance of the segmentation software should also be investigated for different types of liver tumors (i.e. neuroendocrine, colorectal, etc. cancers), for different intra-arterial therapies (i.e. drug-eluting beads and radioembolization), and at additional follow-up imaging time points (here a differential segmentation between enhancing and non-enhancing portions of the lesion could help identify the effect of sequential TACEs). Third, the target lesion size may change slightly between CE-MRI, CBCT and MDCT because the imaging was done at different time points. However, this difference is not statistically significant due to the embolic nature of intra-arterial therapy; the lesion size may not change much at all after treatment (9, 10). Fourth, many lesions were small. A large variation in tumor sizes could help to mitigate any bias due to lesion size. However, large lesions often have incomplete Lipiodol uptake, making the delineation between lesion and surrounding healthy liver tissue challenging on MDCT because it is a dry, non-contrast enhanced scan.

CONCLUSIONS

To our knowledge, this is the first clinical study to measure the concordance of a 3D semiautomatic tumor volume segmentation in three imaging modalities. A semi-automated 3D segmentation of HCC lesions treated with TACE provides high volumetric concordance across all tested imaging modalities. This can be helpful for volumetric hepatic tumor assessment.

Acknowledgments

Support for this work was provided by NIH/NCI R01 CA160771, P30 CA006973, Philips Research North America, Briarcliff Manor, NY, USA, the Rolf W. Guenther Foundation for Radiological Science, and the Beijing Nova Program (Z121107002512127)

REFERENCES

1. Bruix J, Sherman M. Practice Guidelines Committee AAftSoLD. Management of hepatocellular carcinoma. Hepatology. 2005; 42(5):1208–36. [PubMed: 16250051]
2. Gonzalez-Guindalini FD, Botelho MP, Harmath CB, et al. Assessment of liver tumor response to therapy: role of quantitative imaging. Radiographics : a review publication of the Radiological Society of North America, Inc. 2013; 33(6):1781–800.
3. Vossen JA, Buijs M, Kamel IR. Assessment of tumor response on MR imaging after locoregional therapy. Techniques in vascular and interventional radiology. 2006; 9(3):125–32. [PubMed: 17561215]
4. Kamel IR, Liapi E, Reyes DK, Zahurak M, Bluemke DA, Geschwind JF. Unresectable hepatocellular carcinoma: serial early vascular and cellular changes after transarterial chemoembolization as detected with MR imaging. Radiology. 2009; 250(2):466–73. [PubMed: 19188315]
5. Therasse P, Arbuck SG, Eisenhauer EA, et al. New guidelines to evaluate the response to treatment in solid tumors. European Organization for Research and Treatment of Cancer, National Cancer Institute of the United States, National Cancer Institute of Canada. Journal of the National Cancer Institute. 2000; 92(3):205–16. [PubMed: 10655437]

6. Loffroy R, Lin M, Rao P, et al. Comparing the detectability of hepatocellular carcinoma by C-arm dual-phase cone-beam computed tomography during hepatic arteriography with conventional contrast-enhanced magnetic resonance imaging. Cardiovascular and interventional radiology. 2012; 35(1):97–104. [PubMed: 21328023]
7. Loffroy R, Lin M, Yenokyan G, et al. Intraprocedural C-arm dual-phase cone-beam CT: can it be used to predict short-term response to TACE with drug-eluting beads in patients with hepatocellular carcinoma? Radiology. 2013; 266(2):636–48. [PubMed: 23143027]
8. Chapiro J, Lin M, Duran R, et al. Assessing tumor response after loco-regional liver cancer therapies: the role of 3D MRI. Expert Review of Anticancer Therapy. 2014; 15(2):199–205. [PubMed: 25371052]
9. Pellerin O, Lin M, Bhagat N, Ardon R, Mory B, Geschwind JF. Comparison of Semi-automatic Volumetric VX2 Hepatic Tumor Segmentation from Cone Beam CT and Multi-detector CT with Histology in Rabbit Models. Academic radiology. 2013; 20(1):115–21. [PubMed: 22947274]
10. Tacher V, Lin MD, Chao M, et al. Semiautomatic Volumetric Tumor Segmentation for Hepatocellular Carcinoma: Comparison between C-arm Cone Beam Computed Tomography and MRI. Academic radiology. 2013; 20(4):446–52. [PubMed: 23498985]
11. Lin M, Pellerin O, Bhagat N, et al. Quantitative and volumetric European Association for the Study of the Liver and Response Evaluation Criteria in Solid Tumors measurements: feasibility of a semiautomated software method to assess tumor response after transcatheter arterial chemoembolization. Journal of vascular and interventional radiology : JVIR. 2012; 23(12):1629–37. [PubMed: 23177109]
12. Prasad SR, Jhaveri KS, Saini S, Hahn PF, Halpern EF, Sumner JE. CT tumor measurement for therapeutic response assessment: comparison of unidimensional, bidimensional, and volumetric techniques initial observations. Radiology. 2002; 225(2):416–9. [PubMed: 12409574]
13. Sohaib SA, Turner B, Hanson JA, Farquharson M, Oliver RT, Reznek RH. CT assessment of tumour response to treatment: comparison of linear, cross-sectional and volumetric measures of tumour size. The British journal of radiology. 2000; 73(875):1178–84. [PubMed: 11144795]
14. Bonekamp S, Halappa VG, Geschwind JF, et al. Unresectable hepatocellular carcinoma: MR imaging after intraarterial therapy. Part II. Response stratification using volumetric functional criteria after intraarterial therapy. Radiology. 2013; 268(2):431–9. [PubMed: 23616632]
15. Bonekamp S, Li Z, Geschwind JF, et al. Unresectable hepatocellular carcinoma: MR imaging after intraarterial therapy. Part I. Identification and validation of volumetric functional response criteria. Radiology. 2013; 268(2):420–30. [PubMed: 23616631]
16. Chapiro JWL, Lin M, Cornish T, Wang Z, Geschwind J-F. 3D Evaluation of Tumor Necrosis in HCC Patients after TACE – A Radiologic-Pathologic Correlation. Radiology. 2014
17. Mahr A, Levegrun S, Bahner ML, Kress J, Zuna I, Schlegel W. Usability of semiautomatic segmentation algorithms for tumor volume determination. Investigative radiology. 1999; 34(2): 143–50. [PubMed: 9951794]
18. Ray S, Hagge R, Gillen M, et al. Comparison of two-dimensional and three-dimensional iterative watershed segmentation methods in hepatic tumor volumetrics. Medical physics. 2008; 35(12): 5869–81. [PubMed: 19175143]
19. Yim PJ, Vora AV, Raghavan D, et al. Volumetric analysis of liver metastases in computed tomography with the fuzzy C-means algorithm. Journal of computer assisted tomography. 2006; 30(2):212–20. [PubMed: 16628034]
20. Zhao B, Schwartz LH, Jiang L, et al. Shape-constraint region growing for delineation of hepatic metastases on contrast-enhanced computed tomograph scans. Investigative radiology. 2006; 41(10):753–62. [PubMed: 16971799]
21. Hermoye L, Laamari-Azjal I, Cao Z, et al. Liver segmentation in living liver transplant donors: comparison of semiautomatic and manual methods. Radiology. 2005; 234(1):171–8. [PubMed: 15564393]

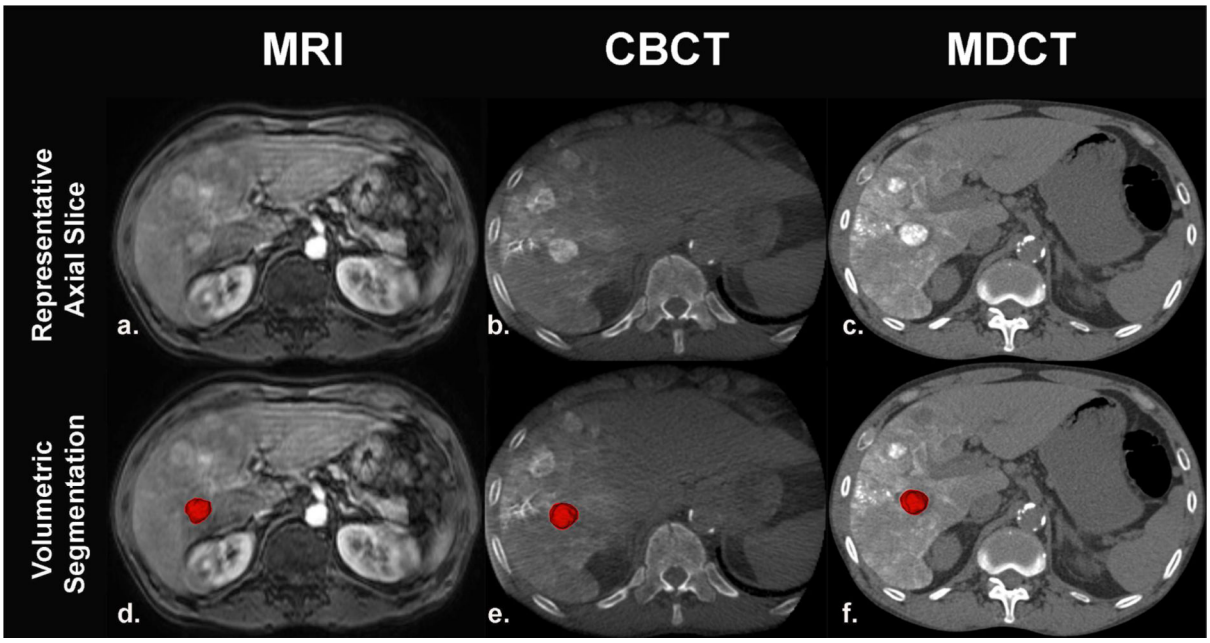

Figure 1.

Three-dimensional semiautomatic segmentation of tumor in HCC on a representative case. Tumor at representative axial slice level was visualized well on CE-MRI, DP-CBCT and MDCT (a, b, c). Three-dimensional segmentation volume rendering on the same slice (d, e, f).The tumor volumes on Pre-MRI, CBCT and MDCT were 3.85 cm^3, 4.47 cm^3 and 3.97 cm^3 respectively.

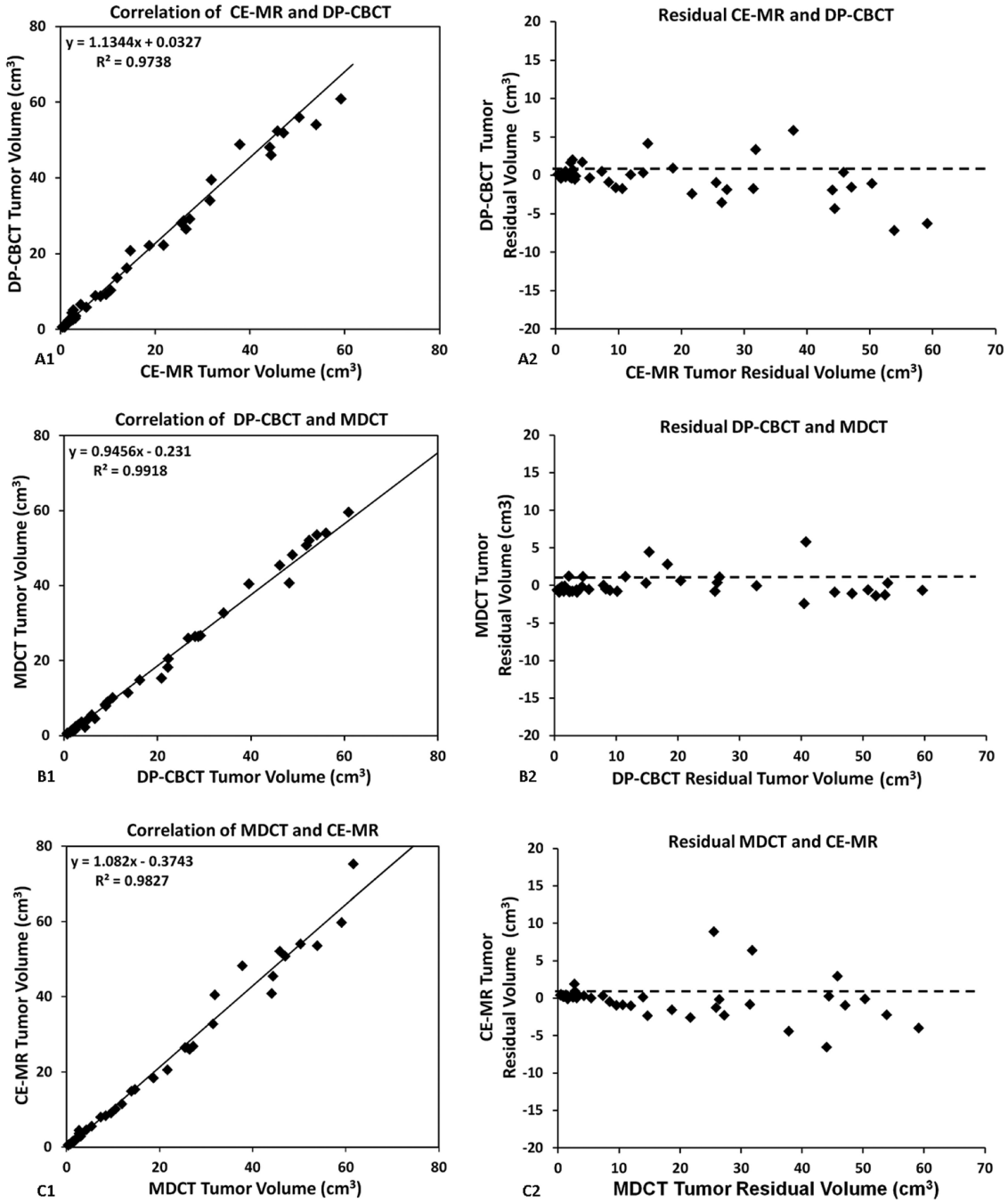

Figure 2.

Comparison of tumor volumes between CE-MR, DP-CBCT and MDCT. (A1,B1,C1) shows the correlation of CE-MR and DP-CBCT,DP-CBCT and MDCT, MDCT and CE-MR. (A2,B2,C2) shows the residual plots between CE-MR,DP-CBCT and MDCT.

Table 1

Tumor volume comparison on three modalities.

Variable	Tumor volume(cm^3)	*P*-value
CE-MR	18.72±19.13	
CBCT	21.26±21.99	0.577
CBCT	21.26±21.99	
MDCT	19.88±20.88	0.770
MDCT	19.88±20.88	
CE-MR	18.72±19.13	0.794

Data were expressed as means ± standard deviations.